Solid State NMR: MAS Imaging & *Path-Sum* for Spin Dynamics

C. Bonhomme*[1], Y. Hammami[1], F. Fayon[2], V. Sarou-Kanian[2], O. Faizy[3], P.-L. Giscard[3]

[1]Sorbonne Université, Paris, France

[2]CEMHTI, Orléans, France

[3]LMPA, Calais, France

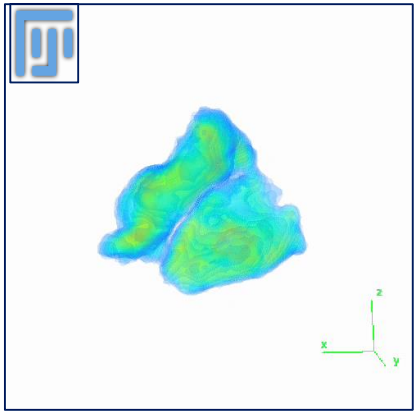

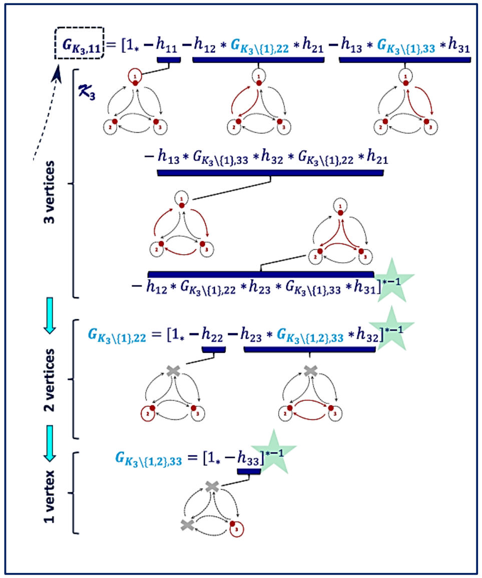

PANACEA

Third Annual User Meeting in Aveiro

Symposium 3 - Solid-state NMR instrumentation, software and other perspectives

■ **SSNMR / Magic Angle Spinning MRI: a unique characterization platform for kidney stones**

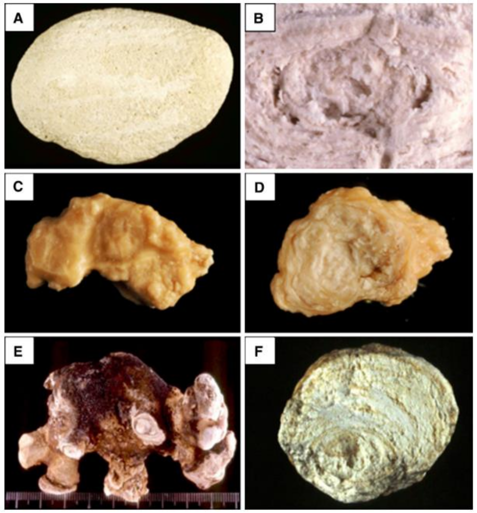

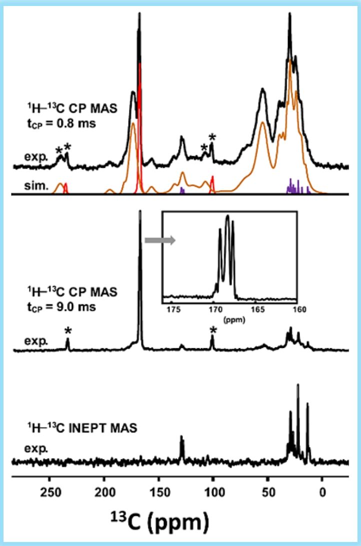

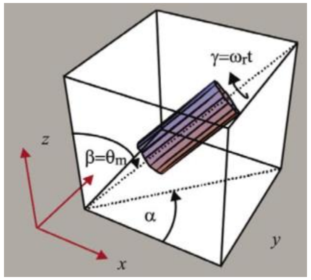

tribute Pampel, Engelke
Bruker

■ **Spin Dynamics: Graph theory, *Path-Sum*, analytical and numerical approaches**

Pathological calcifications (kidney stones, KS)

a major societal/health problem worldwide
(in France, related costs *per year* > 800 million €)

an intrinsic structural/chemical complexity

- **minerals**
- **fatty acids, triglycerides, proteins**
- **… ↔ *hybrids* (organic/inorganic)**

Ca oxalates, CaOx (Mono-, Di-, Trihydrate)
Ca, Mg phosphates (hydroxyapatite, brushite, struvite…)

CaOx

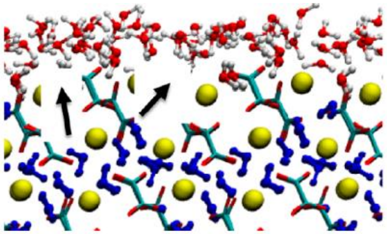

HAp

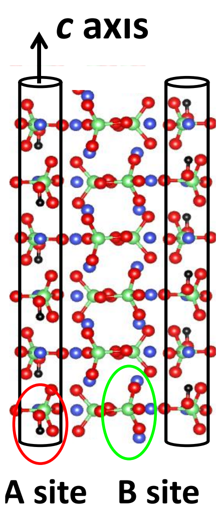

Coll.: M. Daudon, E. Letavernier, D. Bazin
(Tenon hospital, Paris)

Bonhomme *et al.*, Magn. Res. 2021

More complexity

► MRI?

"… Using *standard* MRI technique, stones appear as a non-specific void…"

(Brisbane, Nat. Rev. Urol., 2016)

► state of the art (hospitals): µ–Computed Tomography (CT)

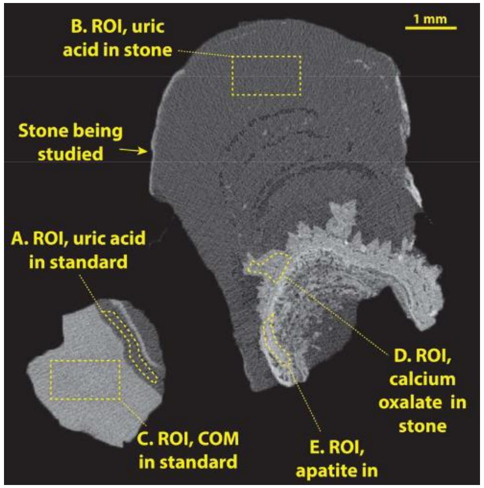

various CaOx?

drug-induced KS, gels, non-radio opaque phases?

relative lack of chemical information

Question @Tenon: "3D information with chemical content?"

First MAS MR Images of kidney stones: Chemical Shift Imaging

Coll.: V. Sarou-Kanian, F. Fayon, Orléans , France (Pampel, Engelke, …
M. Yon *et al*., 2017)

rotating pulsed field gradients

brushite +++

organics +

No HAp…

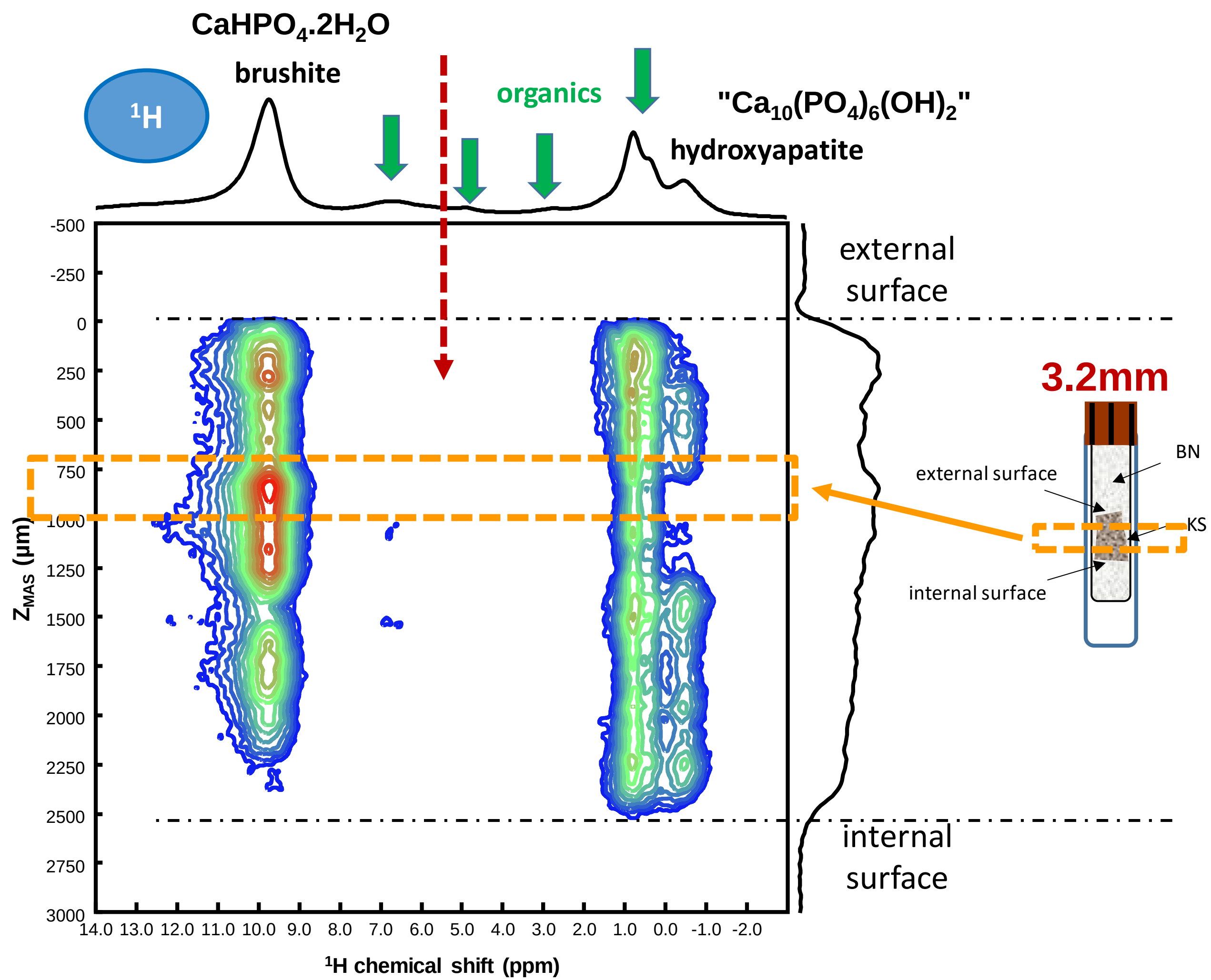

First MAS Images of kidney stones: Chemical Shift Imaging

WB 750 MHz AVANCE III HD, 17.6 T. Bruker *Micro 2.5*. 2.5 $G.cm^{-1}A^{-1}$ (60 A per axis). 3.2mm Bruker probe (up to 24 kHz). FOV ~ 3.5 mm. Res. ~ 31 μm, 61μm.

see: Pampel, 2006, Sarou-Kanian, 2015, Maudsley *et al*., 1982
***spectral* dim.: direct**
***spatial* dim.: indirect**

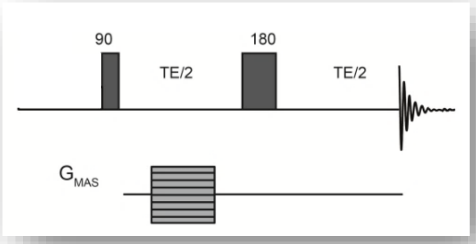

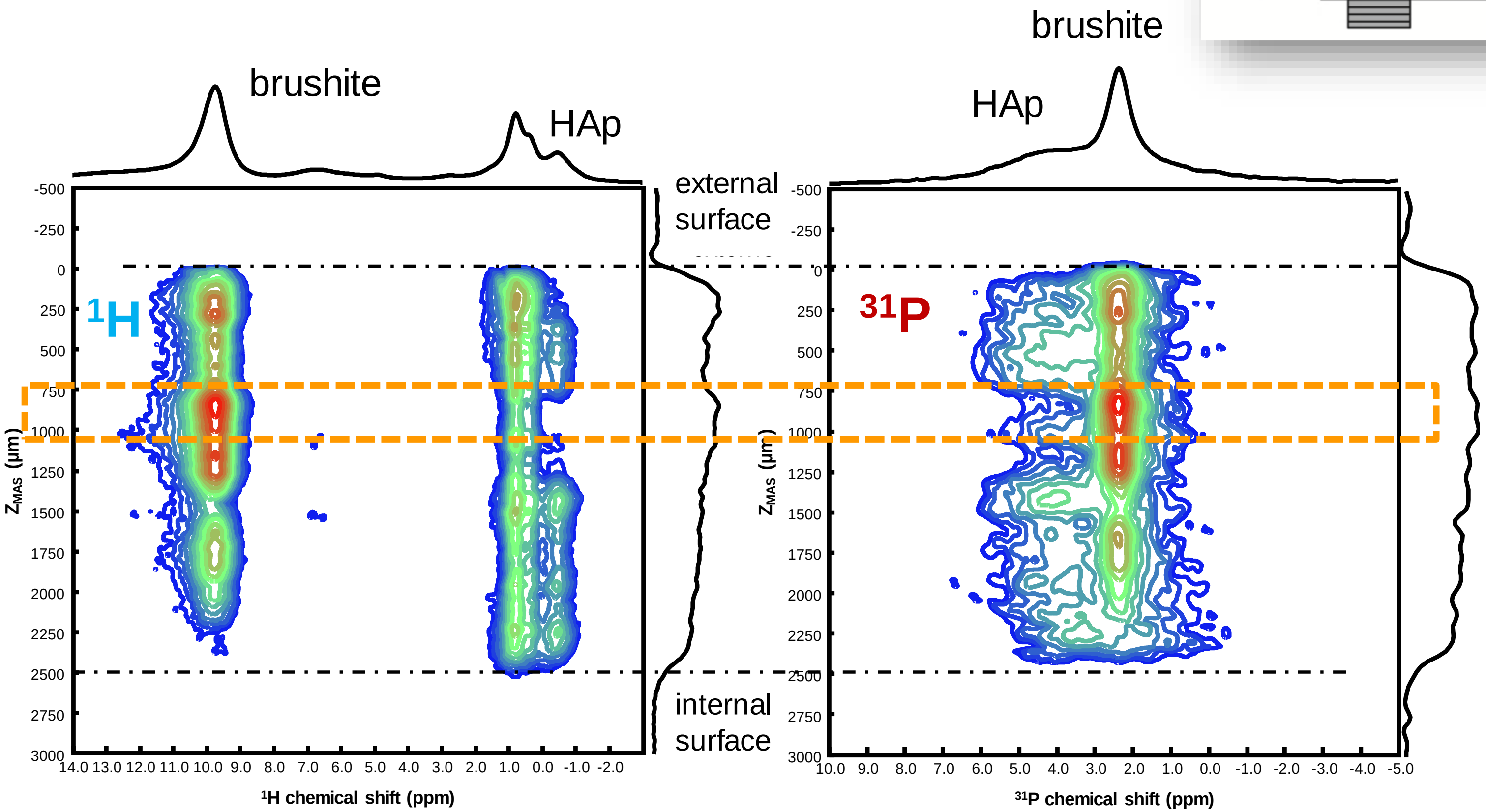

3D images (June 2024, Orléans)

"Organic" sample : **T86891**
60% **proteins (P)** / 30% **triglycerides (TG)** / 10% apatite

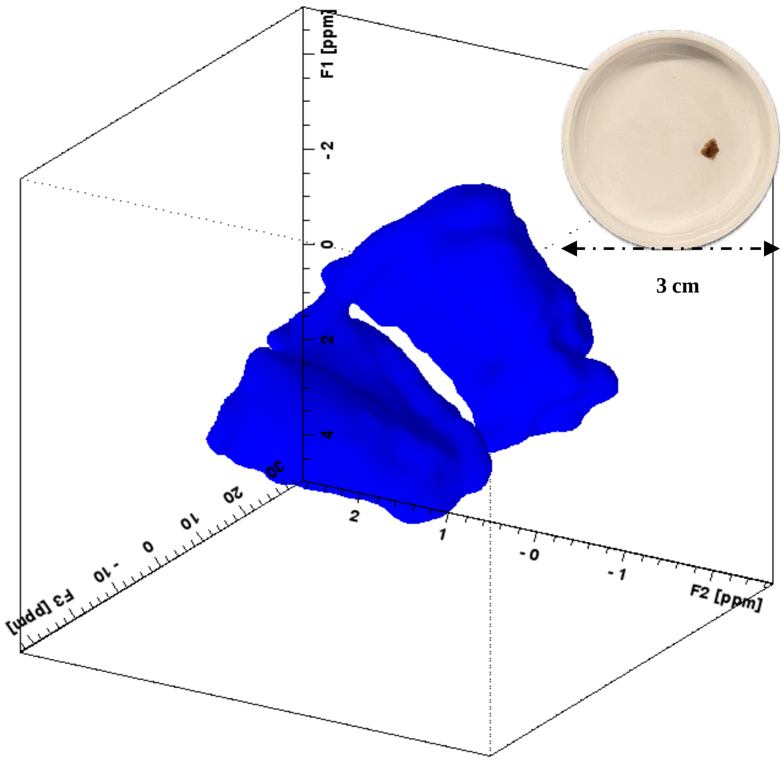

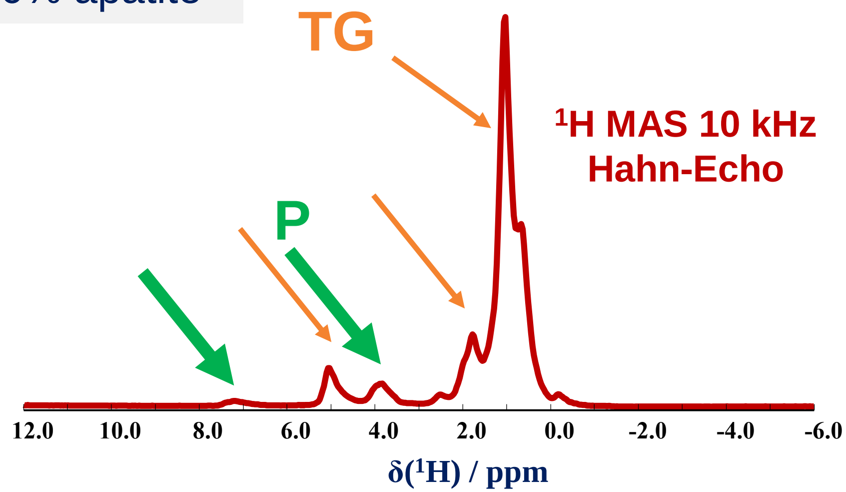

3D ^{1}H MAS MRI (10 kHz),
image size ***4x4x4mm***

40x75x75 µm

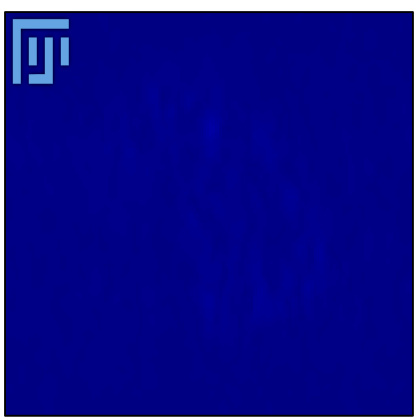

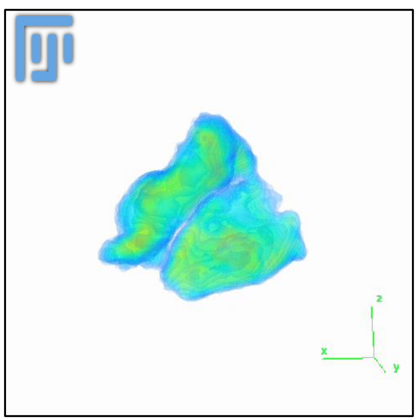

FIJI 3D reconstruction

3D images (June 2024, Orléans)

"Inorganic" sample : **T83936**
87% **struvite (S)** / 10% apatite / 3% proteins

$NH4MgPO_4.6H_2O$

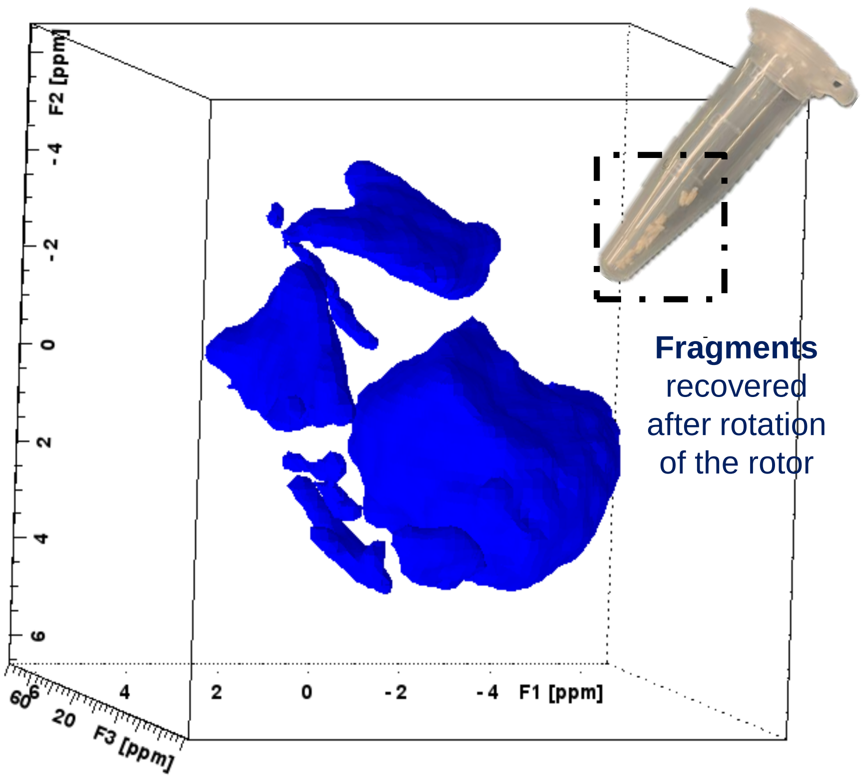

3D ^{1}H–^{31}P MAS MRI (10 kHz),
image size ***5x4x4mm***

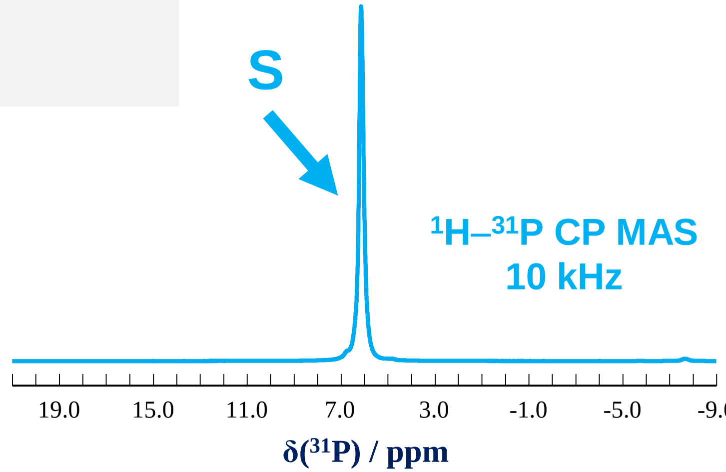

50x150x150 µm

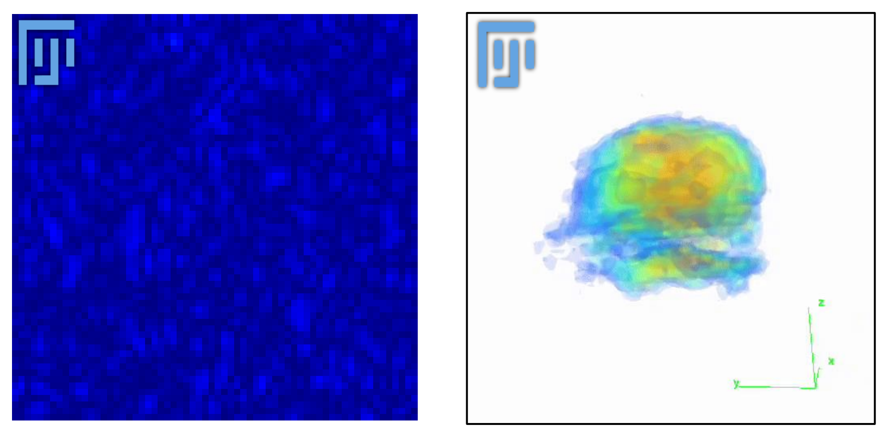

FIJI 3D reconstruction

Outline

■ SSNMR / Magic Angle Spinning MRI: a unique characterization platform for kidney stones

Question @Tenon: "3D information with chemical content?"

■ **Spin Dynamics: Graph theory, *Path-Sum*, analytical and numerical approaches**

Adjacency *finite* matrix $A_{\mathcal{G}}$

$$A_{\mathcal{G}} = \begin{pmatrix} a_{11} & a_{12} & a_{13} \\ a_{21} & a_{22} & a_{23} \\ 0 & a_{32} & 0 \end{pmatrix}$$

⬇

entry: ***weight*** on a ***directed edge***

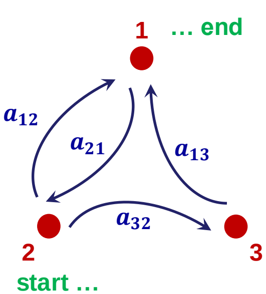

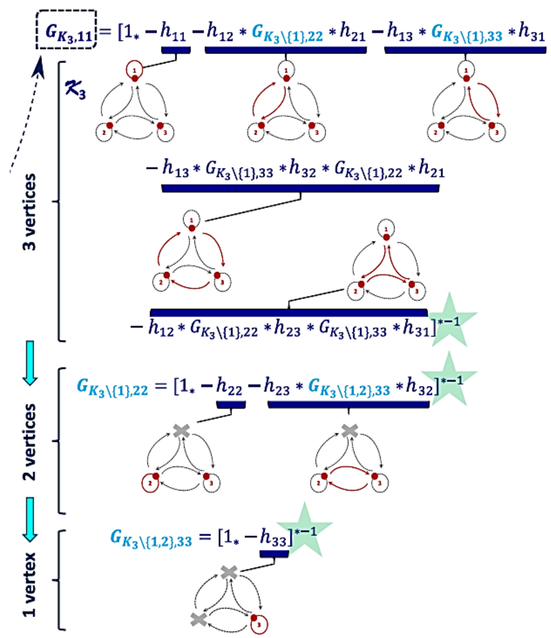

The evolution operator U(t) and the ordered exponential

Dyson time-ordering operator

$$\hat{U}(t',t) = \mathrm{OE}\left[-i\hat{H}(t',t)\right] = \hat{T}\exp\left(-i\int_{t}^{t'}\hat{H}(\tau)d\tau\right)$$

Magnus

Floquet

G. Floquet, *Ann. Sci. Ecole Norm. Sup*., 1883

F.J. Dyson, *Phys. Rev*., 1949

W. Magnus, *Pure Appl. Math*., 1954

F. Fer, *Bull. Classe Sci. Acad. Roy. Bel*., 1958

J.H. Shirley, *Phys. Rev*., 1965

U. Haeberlen, J.S. Waugh, *Phys. Rev*., 1968

M.M. Maricq, *Phys. Rev*., 1982

S. Vega, E.T. Olejniczak, R.G. Griffin, *J. Chem. Phys*., 1984

I. Scholz, B.H. Meier, M. Ernst, *J. Chem. Phys*., 2007

M. Leskes, P.K. Madhu, S. Vega, *Progress in NMR Spect*., 2010

M. Goldman, P. J. Grandinetti, A. Llor *et al., J. Chem. Phys*. 1992

E.S. Mananga, *Solid State NMR*, 2013

K. Takegoshi, N. Miyazawa, K. Sharma, P. K. Madhu, *J. Chem. Phys*., 2015

M. Chavez, M. Ernst 2023

perturbative methods, periodic,… convergence (?)

Ordered exponential and Path-Sum

Adjacency *finite* matrix $\mathbf{A}_{\mathcal{G}}$

$$\mathbf{A}_{\mathcal{G}} = \begin{pmatrix} a_{11} & a_{12} & a_{13} \\ a_{21} & a_{22} & a_{23} \\ 0 & a_{32} & 0 \end{pmatrix}$$

entry: ***weight*** on a ***directed edge***

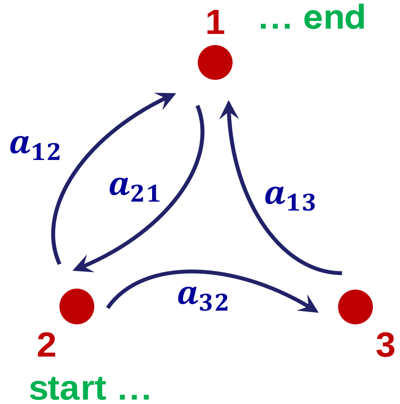

$$\boldsymbol{OE}\left[A_{\mathcal{G}}\right](\boldsymbol{t}',\boldsymbol{t}) = \left(\begin{array}{c} \cdots \\ <\boldsymbol{s}_j \left|\boldsymbol{OE}[A_{\mathcal{G}}](\boldsymbol{t}',\boldsymbol{t})\right| \boldsymbol{s}_i > \\ \cdots \end{array} \right)$$

Path-Sum

▶ resummation of all $\mathcal{W}$ involves a ***finite*** number of operations: ***sum** on **simple paths*** and ***continuous fraction** of **simple cycles*** with vertex removal

Giscard, *J. Math. Phys.*, 2015

Time dependent 2×2 matrix

$$(f * g) = \int_t^{t'} f(t',\tau)g(\tau,t)d\tau$$

OE[A](t',t) = $\begin{pmatrix} \int_t^{t'} G_{K_2,11}(t',\tau)d\tau & OE_{12}(t',t) \\ OE_{21}(t',t) & \int_t^{t'} G_{K_2,22}(t',\tau)d\tau \end{pmatrix}$

$a_{ij}(t)$

$$[1_* - (* \quad * \quad * \cdots)]^{*-1} = \sum_{n\geq 0} (* \quad * \quad * \cdots)^{*n}$$

► Neumann series

Kernel, K

continuous fraction on *simple cycles*

$$G_{K_2,11} = [1_* - a_{11} - a_{12} * G_{K_2\backslash\{1\},22} * a_{21}]^{*-1}$$

$\mathcal{K}_2$

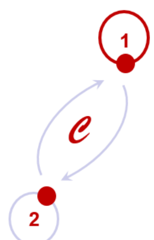

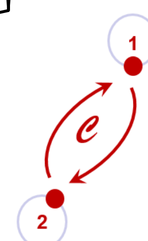

$$G_{K_2\backslash\{1\},22} = [1_* - a_{22}]^{*-1}$$

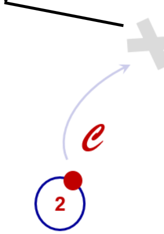

$$OE_{12}(t',t) = \int_t^{t'} G_{K_2\backslash\{2\},11} * a_{12} * G_{K_2,22}(t',\tau)d\tau$$

sum on *simple paths*

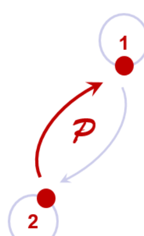

► END !

► ***finite*** sum on simple $\mathcal{P}$

► END of the ***continued fraction*** !

► ***finite*** sum on $\mathcal{C}$

Some results

Path-Sum solution

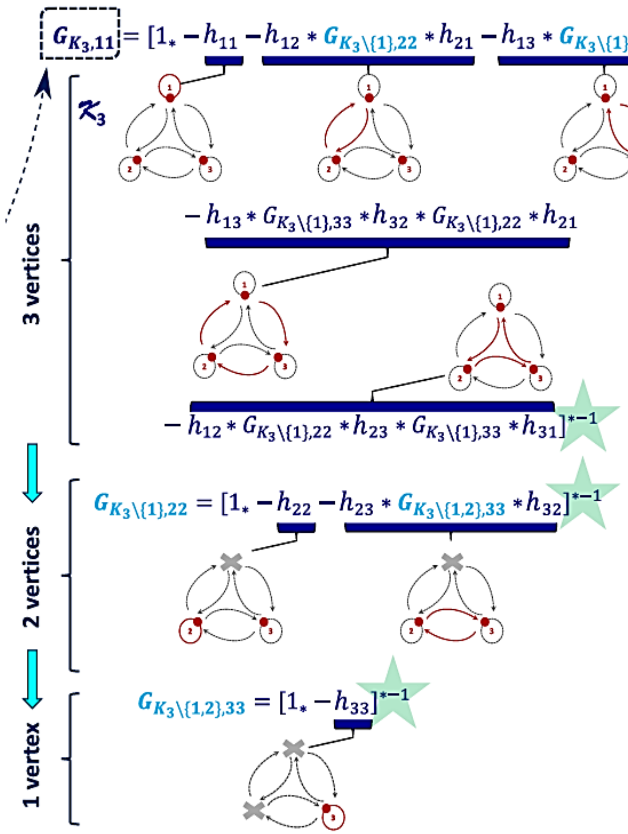

► exact representation (transcendent, special functions…)

► non perturbative, super exponentially CV

► always closed form in

$$[1_* - (* \quad * \quad * \cdots)]^{*-1}$$

► Neumann series: analytic, closed form at fixed accuracy

Linearly polarized excitation, Bloch-Siegert (BS) effect

$$\mathbf{H}(t) = \begin{pmatrix} \frac{\omega_0}{2} & 2\beta\cos(\omega t) \\ 2\beta\cos(\omega t) & -\frac{\omega_0}{2} \end{pmatrix}$$

► visualizing the solution at analytical / numerical level

P(t) transition probability

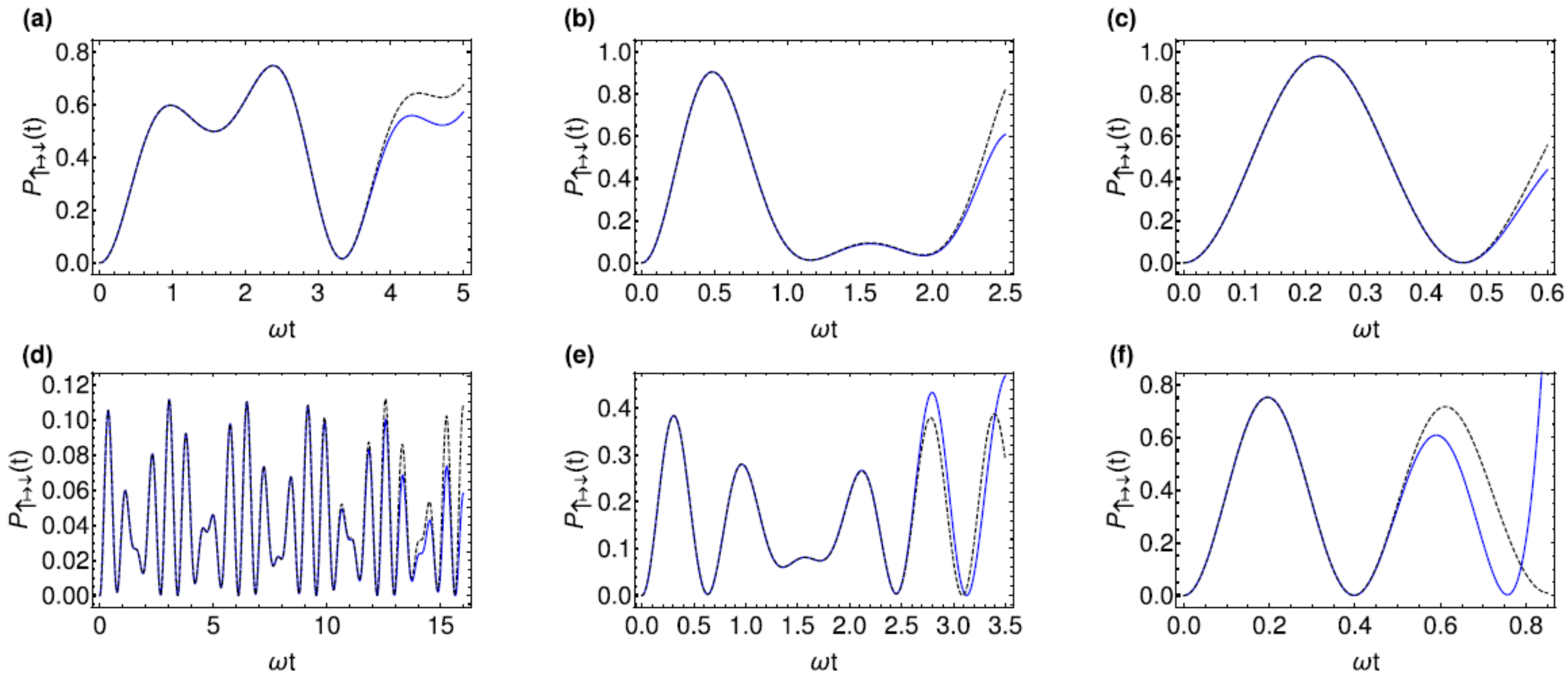

ON and OFF resonance

$\beta/\omega \ll 1$ *weak*

$\beta/\omega \gg 1$ *strong*

Giscard, Bonhomme, *Phys. Rev. Res.*, 2020

Linearly polarized excitation, Bloch-Siegert (BS) effect

$$\mathbf{H}(t) = \begin{pmatrix} \frac{\omega_0}{2} & 2\beta\cos(\omega t) \\ 2\beta\cos(\omega t) & -\frac{\omega_0}{2} \end{pmatrix}$$

► analytical formula

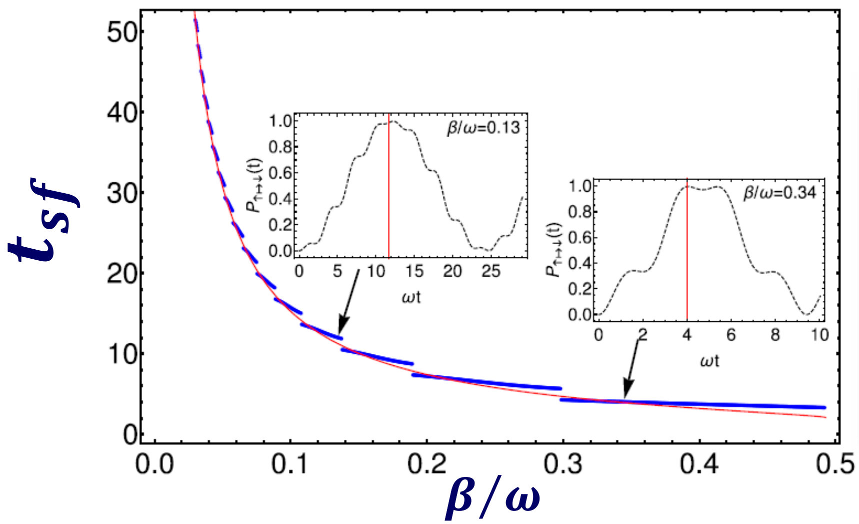

spin flip duration, t_{sf}

$$t_{sf} = \frac{1}{2\sqrt{2}}\sqrt{\frac{12}{\beta^2} - \frac{15}{\omega^2} + \frac{\sqrt{3}}{\beta^4\omega^2}\sqrt{91\beta^8 - 88\beta^6\omega^2 + 16\beta^4\omega^4}}$$
$$= \frac{1}{\beta}\sqrt{\frac{1}{2}(3+\sqrt{3})} - \frac{\beta}{8\omega^2}\sqrt{\frac{1}{2}(129+67\sqrt{3})}$$
$$- \frac{\beta^3}{128\omega^4}\sqrt{\frac{1}{2}(16131+5545\sqrt{3})} + O(\beta^4). \qquad (11)$$

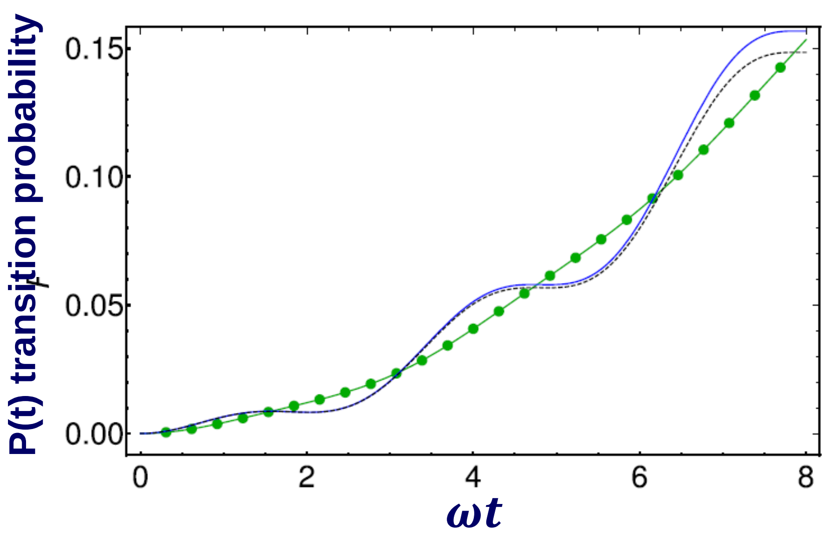

$\beta/\omega \ll 1$

order 0 of the Path-Sum solution

$$G_{\uparrow}^{(0)} = \delta(t', t)$$

$$P_{\uparrow\to\downarrow}^{(0)}(t) = \frac{\beta^2 t}{\omega}\sin(2\omega t) + \frac{\beta^2}{2\omega^2} + \beta^2 t^2 - \frac{\beta^2}{2\omega^2}\cos(2\omega t).$$

Linearly polarized excitation, Bloch-Siegert (BS) effect

$$\mathbf{H}(t) = \begin{pmatrix} \frac{\omega_0}{2} & 2\beta\cos(\omega t) \\ 2\beta\cos(\omega t) & -\frac{\omega_0}{2} \end{pmatrix}$$

$$\mathsf{H}_0 = (\omega_0/2)\sigma_z, \; \mathsf{H}_1 = 2\beta\cos(\omega t)\sigma_x$$

Bi-FRAME transformation

$$\mathsf{U}^{[m]}_{\text{bi-frame}} := \mathsf{U}_0 \star \sum_{k=0}^{m} \mathcal{A}^{\star k} \star \mathsf{G}_1$$

$$\mathcal{A}(t,s) = \beta\omega_0 \cos(\omega t)\cos\left(\frac{2\beta}{\omega}\sin(\omega t)\right)\begin{pmatrix} -iS(t,s) & \overline{C}(t,s) \\ -C(t,s) & i\overline{S}(t,s) \end{pmatrix} + \beta\omega_0\cos(\omega t)\sin\left(\frac{2\beta}{\omega}\sin(\omega t)\right)\begin{pmatrix} iC(t,s) & \overline{S}(t,s) \\ -S(t,s) & -i\overline{C}(t,s) \end{pmatrix}$$

$$S(t,s) := e^{\frac{1}{2}i\omega_0 s}\int_s^t e^{-\frac{1}{2}i\omega_0\tau}\sin\left(\frac{2\beta}{\omega}\sin(\omega\tau)\right)d\tau$$

$$C(t,s) := e^{\frac{1}{2}i\omega_0 s}\int_s^t e^{-\frac{1}{2}i\omega_0\tau}\cos\left(\frac{2\beta}{\omega}\sin(\omega\tau)\right)d\tau$$

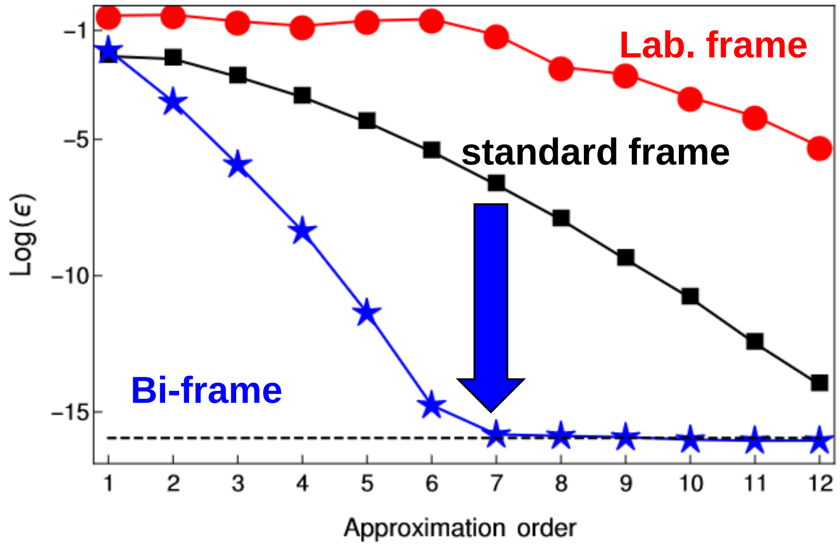

$$\omega_0/\omega = 2/3$$

$$\beta/\omega = 8/15$$

Giscard, *J. Integral Equations Appl*. 2020
Giscard, Bonhomme, *Phys. Rev. Res*. 2020
Giscard, Faizy, Bonhomme, 2024 *in prep*.

Conclusions and acknowledgments

- **MAS MRI: a new tool for diagnosis at hospitals?**
- ***Path-Sum*: new analytical & numerical insight in spin dynamics**

Y. Hammami

M. Daudon, E. Letavernier, D. Bazin (Tenon Hospital)

V. Sarou-Kanian, F. Fayon

O. Faizy, P.-L. Giscard

anr